

Vibrational Excitations of Charged Solitons in Polyacetylene

Eugene J. Mele and Michael J. Rice

Xerox Webster Research Center, Webster, New York 14580

(Received 14 February 1980)

Theoretical studies of the vibrational excitations of charged solitons in polyacetylene are reported. Two strongly infrared active modes, derived from bulk optical phonons, are associated with these defects and we suggest the presence of a third, as yet unobserved, infrared-active mode in the acoustic phonon regime.

PACS numbers: 78.30.Jw, 78.50.-w, 63.20.Dj

Following the demonstrations of controlled conductivity over twelve orders of magnitude with doping¹ and of semiconducting properties at low doping levels,² polyacetylene [(CH)_x] has received considerable scientific attention. It has also been realized that one-electron theory [if applicable to (CH)_x] predicts that the lightly doped polymer should differ qualitatively from the usual picture of a lightly doped semiconductor.^{3,4} Within such a theory, one concludes that the transfer of an electron to or from the polymer does *not* result in a hydrogenic impurity state or even an unbound carrier in the valence or conduction bands. Rather, the excess carrier is predicted to be accommodated in a soliton (or π phase kink), an extended lattice defect across which the sign of the bond alternation is reversed.^{3,4} Neglecting correlations each such defect may be shown to introduce a half-filled state at midgap when neutral, which may then accommodate the excess electron or hole in a diamagnetic center when charged. Despite its success in explaining the reduced strength of the Curie tail in the magnetic susceptibility of the lightly doped polymer,⁵ the soliton model has not gained universal acceptance.⁶ In this Letter, we report an investigation of the vibrational structure of solitons in (CH)_x and readdress the question of whether charged solitons occur in the lightly doped polymer. In the frequency regime which has to this point been experimentally studied we find several internal modes peculiar to such defects. Two of these are remarkably, strongly infrared active, deriving their oscillator strength from interactions with the π electrons, and would be observable at very low doping

levels. We suggest that these two modes have, in fact, been observed in experiments which correlate changes in the infrared absorption of these films with light doping.⁷ The expected infrared activity associated with the pinning of the mobile charged soliton to an ionized impurity does not occur in this frequency regime; on the basis of studies of a continuum model³ and a discrete lattice model⁴ for these defects, we anticipate that such absorption will ultimately be observed at much lower frequency, i.e., in the acoustic phonon regime.

To describe the vibrations of the polymer we have constructed a force-field model which consists of two principal parts. First, "bare" nearest-neighbor bond-stretching and bond-bending force constants are chosen by inspecting the characteristic vibrations of small organic complexes containing double and single C-C bonds.⁸ We interpolate dependence of the bond-stretching force constants on bond length⁹ to define the force constants appropriate for the infinite polyene, and the force field thus derived is cast into the form of a Born Hamiltonian from which the bare phonons of the polyene chain are calculated. Second, we include a set of delocalized force constants derived from interactions of atomic displacements with the extended π electronic states. The importance of this electronic susceptibility for determining polyene phonon frequencies, especially those of the backbond stretching vibrations, has been discussed in the chemical literature.¹⁰⁻¹² We express this effect as a correction to the bare dynamical matrix, $\delta L_{\mu\nu}$, coupling displacements μ and ν with wave vector q given by:

$$\delta L_{\mu\nu}(q) = 2 \sum_k \frac{\langle n, k | V_{\mu}^*(q) | n', k+q \rangle \langle n', k+q | V_{\nu}(q) | n, k \rangle}{E_{n', k+q} - E_{n, k}}, \quad (1)$$

where $V_{\mu}(q)$ denotes a modulation of the electronic Hamiltonian linear in the displacement $\mu(q)$ and the $|n, k\rangle$ ($|n', k\rangle$) are the filled (empty) eigenstates in the π manifold with eigenvalues $E_n(k)$ [$E_{n'}(k)$]. The V_{μ} are completely defined by the geometry of the chain and a constant, β , the derivative of the nearest-

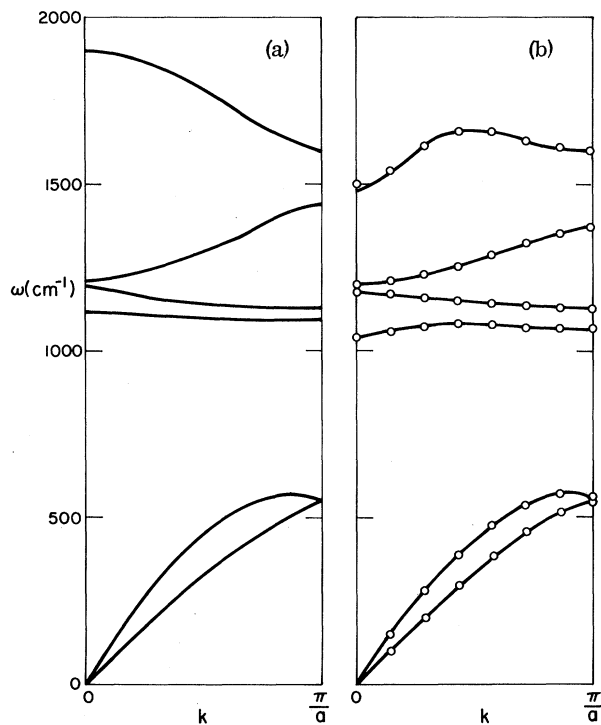


FIG. 1. Left panel: In-plane vibrations below 2000 cm^{-1} in *trans*-(CH) $_x$ calculated from the bare-force-field model. Right panel: Phonons calculated including coupling to π electrons (solid curve); phonons obtained by truncating the delocalized force field after sixth nearest neighbors (open circles).

neighbor π -electron transfer integral with respect to bond length.¹³ β is empirically adjusted to bring the screened long-wavelength C-C and C=C stretching modes in the infinite polyene into good agreement with the principal Raman peaks observed near ~ 1474 and $\sim 1080 \text{ cm}^{-1}$.¹⁴⁻¹⁶ Thus the data depicted in the right panel of Fig. 1 are obtained by screening the bare phonons of the left panel with $\beta = 8 \text{ eV/\AA}$. This implies a 1.2-eV wide Peierls gap, in reasonable agreement with the 1.4 eV optical absorption threshold observed experimentally. We require a truncation of the matrix $\delta L_{\mu\nu}$ in coordinate space in order to study the kink in an infinite chain; the open circles in Fig. 1(b) demonstrate the good convergence we obtain by retaining terms in $\delta L_{\mu\nu}$ up to sixth nearest neighbors.

Finally, the coupling between the backbone modes and the π electrons will, in general, introduce into the electronic optical response functions, in addition to the usual interband response, terms in which density fluctuations in the π electron gas are coupled through the phonons.¹⁷⁻¹⁹

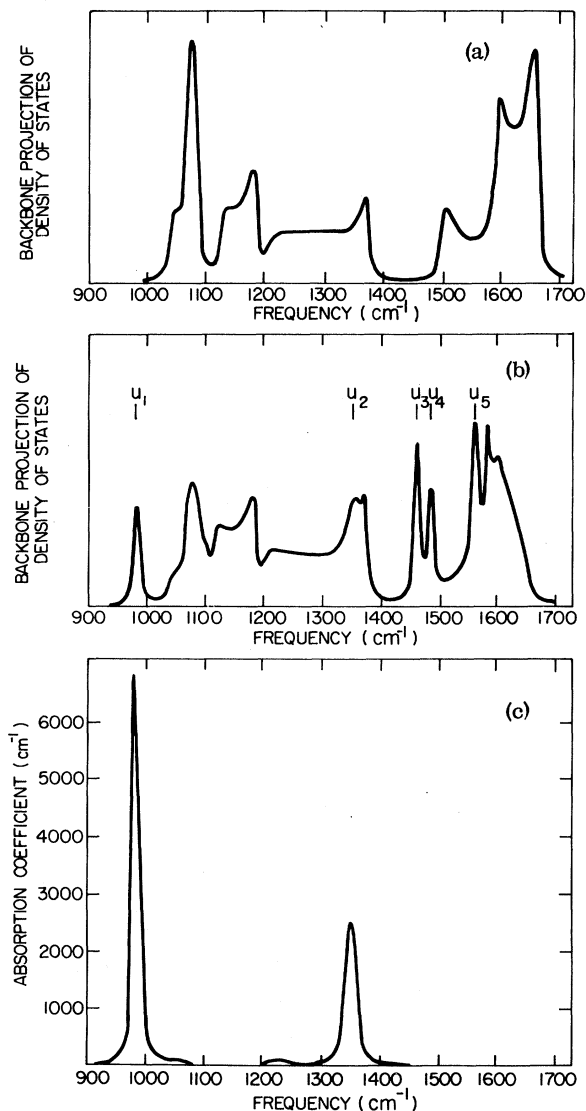


FIG. 2. (a) Projected phonon density of states (PDOS) for carbon motions in *trans*-(CH) $_x$; (b) PDOS averaged over a 15-atom section containing a soliton; (c) absorption coefficient calculated for 10^{19} cm^{-3} of such defects.

This phonon induced contribution to the electronic polarizability rigorously vanishes for the neutral chain since no modulation of the nearest-neighbor one-dimensional Hamiltonian can provide a net migration of charge in the neutral chain. For the charged chain, and in particular for the charged soliton in the chain, this mechanism associates a massive oscillator strength with the ungerade internal vibrations of the defect, as we will show.

In Fig. 2(a) we show the density of modes of a perfect *trans*-(CH) $_x$ chain projected on to the carbon displacements.²⁰ The critical points associ-

ated with the phonon bands of Fig. 1(b) are apparent. Between 1000 and 1200 cm^{-1} we see that the skeletal modes are hybridized with H bending motions. The structure between 1200 and 1400 cm^{-1} is assigned to oscillations dominated by C-C stretching character, those between 1500 and 1700 cm^{-1} are dominated by C=C stretching motions.

Turning to the chain containing a soliton, we recognize that the defect introduces two new considerations for the local vibrational structure. First the "bare" force constants are modified as the magnitude of the bond alternation progresses smoothly through zero, changing sign at the center of the defect. Thus one anticipates vibrational modes characteristic of order " $1\frac{1}{2}$ " bonds localized in the defect. Secondly, in the vicinity of the kink the electronic structure is altered, and hence the electronic contribution to the dynamical matrix $\delta L_{\mu\nu}$ is locally modified. This latter effect causes a general increase in the magnitudes of these corrections in the kink; explicit calculation for the case considered below shows $\sim 20\%$ increase in the diagonal corrections in the center of the defect as compared with the crystalline values. To study the roles of the two processes we have embedded a charged soliton with half width $l=5$ bond lengths (same convention as in Ref. 4) in a 15-atom cluster whose ends are matched to semi-infinite crystalline chains. The electronic corrections to the dynamical matrix are calculated to convergence within the same 15-atom section from the eigensolutions of infinite electronic Hamiltonian. All other screening matrix elements, i.e., those away from the kink, retain their bulk values. Finally the vibrational structure of the central 15-atom section of the infinite chain is numerically evaluated by applying a Green's-function formalism to the dynamical matrix.

Figure 2(b) shows the local density of modes obtained in this calculation summed over carbon displacements in the 15-atom unit containing the kink.²⁰ The vertical bars labeled u_1 - u_5 denote the pronounced defect-related local modes. The modes u_1 at 980 cm^{-1} and u_2 at 1360 cm^{-1} are the two most significant of these. The associated eigenvectors are depicted in Fig. 3 where it is seen that u_1 (u_2) is an ungerade mode with respect to the defect center which projects onto bond-length oscillations of the weaker (stronger) bonds as one proceeds away from the defect center. The displacements of more distant atoms in the u_1 mode will clearly tend to zero whereas u_2 ,

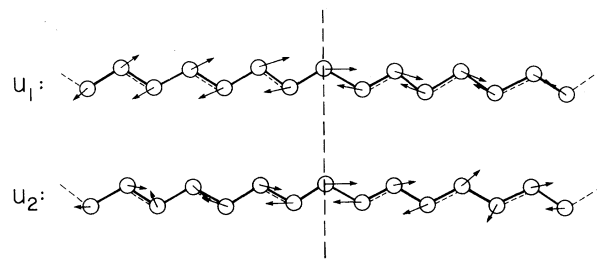


FIG. 3. Normal modes for the u_1 and u_2 vibrations. The vertical dashed line marks the center of the soliton with the even bonds as counted from the center becoming increasingly strong.

a resonant mode, presumably evolves into a bulk-like vibration. Each mode is shifted from the frequencies of bulk modes of similar character because of the enhanced polarizability of the π electrons in the defect.

The significance of u_1 and u_2 is apparent in Fig. 2(c) where we have plotted the absorption coefficient associated with a density of 10^{19} cm^{-3} of these defects in an unoriented film. To obtain these data we have calculated, with the random-phase approximation, the phonon coupling to density fluctuations in the π -electron gas. As is evident in Fig. 2(c) the two modes u_1 and u_2 are remarkably infrared active. The massive oscillator strength associated with these modes may be understood as resulting from oscillations of the excess charge in the defect level in response to the lattice vibration. Upon closer inspection it is seen that the eigenvectors u_1 and u_2 displayed in Fig. 3 describe an overall contraction of the weaker and stronger bonds, respectively, on one side of the defect and an overall expansion on the other, thus driving charge back and forth across the defect center. We calculate that $\sim 20\%$ of the oscillator strength associated with the added charge is exhausted in these vibrational excitations, with the integrated oscillator strength of the 980-cm^{-1} mode 40% stronger than that of the 1360-cm^{-1} line.

The two defect modes obtained in this calculation are well correlated with the dopant-induced infrared activity in $(\text{CH})_x$ reported by Fincher *et al.*⁷ These experiments associate a strong narrow absorption at 1370 cm^{-1} and a broader, somewhat stronger absorption near $\sim 900\text{ cm}^{-1}$ with light doping of $(\text{CH})_x$ with variety of donors and acceptors. Moreover, the integrated oscillator strengths of the observed features agree to within factors of 2-3 with those predicted in this model, normalized to an equivalent density of do-

nors or acceptors, and indeed without such a vibronic coupling these effects would not be easily discernible at such low doping levels.

It is apparent that this model poorly characterizes the widths of these defect modes. We attribute this deficiency to our theoretical constraint that the soliton be centered at a fixed position in the chain. In the true system the soliton, though bound to an ionized impurity, is mobile, executing zero-point motion in its ground state, and oscillating in response to an applied time-dependent field. Such oscillations will introduce time-dependent fluctuations in the dynamical matrix we have studied and thus we anticipate that the effect of such motions is to introduce a finite lifetime in the normal modes we have discussed.

Finally, we note that the oscillation of the charged soliton bound to an ionized impurity should be associated with its own characteristic infrared activity.^{3,4} As the inertial mass of the defect is quite small [(6–10) m_e] these too should be observable at low doping levels. Calculations based on a continuum model for these solitons²¹ consistently predict that this mode will occur at ~ 300 – 500 cm^{-1} , i.e., at much lower frequency than has been investigated experimentally. Thus the observation of a third infrared-active mode in the acoustic phonon regime should further support the presence of mobile charged solitons in lightly doped (CH)_x.

We thank R. Laughlin and D. Vanderbilt for helpful suggestions.

¹C. K. Chiang, C. R. Fincher, Y. W. Park, A. J. Heeger, H. Shirakawa, E. J. Louis, S. C. Gau, and A. G. MacDiarmid, *Phys. Rev. Lett.* **39**, 1098 (1977).

²C. K. Chiang, S. C. Gau, C. R. Fincher, Y. W. Park, A. G. MacDiarmid, and A. J. Heeger, *Appl. Phys. Lett.* **33**, 18 (1978).

³M. J. Rice, *Phys. Lett.* **71A**, 152 (1979).

⁴W. P. Su, J. R. Schrieffer, and A. J. Heeger, *Phys. Rev. Lett.* **42**, 1698 (1979).

⁵B. R. Weinberger, J. Kaufer, A. J. Heeger, A. Pron,

and A. G. MacDiarmid, *Phys. Rev. B* **20**, 223 (1979), and A. J. Epstein, to be published.

⁶Y. Tomkiewicz, T. D. Schultz, H. Broom, T. C. Clarke, and G. B. Street, *Phys. Rev. Lett.* **43**, 1532 (1979).

⁷C. R. Fincher, M. Ozaki, A. J. Heeger, and A. G. MacDiarmid, *Phys. Rev. B* **19**, 4140 (1979).

⁸G. Herzberg, *Infrared and Raman Spectra of Polyatomic Molecules* (D. Van Nostrand Reinhold, New York, 1945).

⁹J. Bart and C. H. MacGillvary, *Acta Crystallogr. Sect. B* **24**, 1569 (1968).

¹⁰C. A. Coulson and H. C. Longuet Higgins, *Proc. Roy. Soc. London, Ser. A* **193**, 457 (1948).

¹¹R. M. Gavin and S. A. Rice, *J. Chem. Phys.* **55**, 1675 (1971).

¹²T. Kakitani, *Prog. Theor. Phys.* **51**, 656 (1974).

¹³Formally $\mu(q) = x_\mu(q) = (1/N^{1/2}) \sum_i \bar{X}_\mu(\mathbf{R}_i) \exp(i\mathbf{q} \cdot \mathbf{R}_i)$, where $x_\mu(\mathbf{R}_i)$ denotes, in turn, each component of the displacement of each atom in the unit cell labeled by lattice translation vector (\mathbf{R}_i) . In this notation, V_μ is the deformation potential due to $\mu(q)$. That is,

$$V_\mu(q) = -(\beta/N^{1/2}) \sum_i \exp(i\mathbf{q} \cdot \mathbf{R}_i) \{ \epsilon_\mu^+(\mathbf{R}_i) [a_n^\dagger a_{n+1} + a_{n+1}^\dagger a_n] + \epsilon_\mu^-(\mathbf{R}_i) [a_n^\dagger a_{n-1} + a_{n-1}^\dagger a_n] \},$$

where the a_n are destruction operators for electrons on site n [which undergoes displacement $x_\mu(\mathbf{R}_i)$] and the $\epsilon_\mu^\pm(\mathbf{R}_i)$ are dot products between the displacement direction and the carbon-carbon directions (\pm) emanating from site n .

¹⁴H. Shirakawa, J. Ito, and S. Ikeda, *Polym. J.* **4**, 460 (1973).

¹⁵S. L. Hsu, A. J. Signorelli, G. Pez, and R. Baughman, *J. Chem. Phys.* **69**, 106 (1978).

¹⁶S. Lefrant, L. S. Lichtman, H. Temkin, D. B. Fitchen, D. C. Miller, G. E. Whitewell, and J. M. Burlitch, *Solid State Commun.* **29**, 1919 (1979).

¹⁷H. J. Schulz, *Phys. Rev. B* **18**, 5756 (1978).

¹⁸M. J. Rice, *Phys. Rev. Lett.* **37**, 36 (1976).

¹⁹P. A. Lee, T. M. Rice, and P. W. Anderson, *Solid State Commun.* **14**, 703 (1974).

²⁰M. J. Rice and E. J. Mele, to be published.

²¹The projected density of modes, $P(\omega)$, is given by $P(\omega) = -(2\omega/\pi) \text{Im} \sum_\alpha G_{\alpha\alpha}(\omega^2)$, where $G(\omega^2) = [-\omega^2 I - \mathcal{L}]^{-1}$. \mathcal{L} is the dynamical matrix, and the sum on α extends over all carbon displacements. That is, $P(\omega)$ represents the density of modes weighted by the squares of the amplitudes of the carbon displacements.